




Article

Cytotoxic Thiodiketopiperazine Derivatives from the Deep Sea-Derived Fungus *Epicoccum nigrum* SD-388

Lu-Ping Chi ^{1,2,3} , Xiao-Ming Li ^{1,2}, Li Li ^{1,2,3}, Xin Li ^{1,2,*}  and Bin-Gui Wang ^{1,2,4,*} 

¹ Key Laboratory of Experimental Marine Biology, Institute of Oceanology, Chinese Academy of Sciences, Nanhai Road 7, Qingdao 266071, China; chiluping@qdio.ac.cn (L.-P.C.); lixmqdio@126.com (X.-M.L.); 15738367975@163.com (L.L.)

² Laboratory of Marine Biology and Biotechnology, Qingdao National Laboratory for Marine Science and Technology, Wenhai Road 1, Qingdao 266237, China

³ University of Chinese Academy of Sciences, Yuquan Road 19A, Beijing 100049, China

⁴ Center for Ocean Mega-Science, Chinese Academy of Sciences, Nanhai Road 7, Qingdao 266071, China

* Correspondence: lixin@qdio.ac.cn (X.L.); wangbg@ms.qdio.ac.cn (B.-G.W.);

Tel.: +86-532-8289-8890 (X.L.); +86-532-8289-8553 (B.-G.W.)

Received: 8 February 2020; Accepted: 11 March 2020; Published: 13 March 2020



Abstract: Four new thiodiketopiperazine alkaloids, namely, 5'-hydroxy-6'-ene-epicoccin G (1), 7-methoxy-7'-hydroxyepicoccin G (2), 8'-acetoxyepicoccin D (3), and 7'-demethoxyrostratin C (4), as well as a pair of new enantiomeric diketopiperazines, (±)-5-hydroxydiphenylalazine A (5), along with five known analogues (6–10), were isolated and identified from the culture extract of *Epicoccum nigrum* SD-388, a fungus obtained from deep-sea sediments (−4500 m). Their structures were established on the basis of detailed interpretation of the NMR spectroscopic and mass spectrometric data. X-ray crystallographic analysis confirmed the structures and established the absolute configurations of compounds 1–3, while the absolute configurations for compounds 4 and 5 were determined by ECD calculations. Compounds 4 and 10 showed potent activity against Huh7.5 liver tumor cells, which were comparable to that of the positive control, sorafenib, and the disulfide bridge at C-2/C-2' is likely essential for the activity.

Keywords: *Epicoccum nigrum*; deep-sea-derived fungus; thiodiketopiperazines; diketopiperazine enantiomers; cytotoxic activity

1. Introduction

Natural products have historically been a rich source of new drugs or drug candidates. Strikingly, deep-sea-derived microorganisms survive under extreme environments, leading to special biological diversity and prolific metabolisms differing from those of terrestrial microorganisms. Recently, deep-sea-sourced microbial natural products have been reported with high hit-rates from bioactivity screening, particularly in the antitumor area [1,2].

Epicoccum nigrum is a chemically distinct fungal species with potential to produce structurally unique secondary metabolites including thiodiketopiperazines (TDKPs) [3,4], polyketides [5], and polysaccharides [6]. Some of these metabolites exhibited intriguing biological properties, such as antimicrobial [3], cytotoxic [4], and antioxidant activities [5,6].

The TDKP derivatives are a family of diketopiperazines which have been isolated from several fungal sources, such as *Epicoccum nigrum* [3], *Exserohilum rostratum* [7], *Penicillium brocae* [8], and *Penicillium adametzioides* [9].

In continuation of our research aimed at discovery of bioactive metabolites from marine-derived microorganisms [10–12], a fungal strain of *Epicoccum nigrum* SD-388 was isolated from a deep-sea

sediment sample collected at a depth of 4500 m. Chemical investigation of the fungus resulted in the isolation of spiroepicoccin A, an unusual spiro-TDKP derivative, whose stereochemistry could not be elucidated by conventional NMR methods and was solved based on residual chemical shift anisotropies [12]. This result encouraged us to perform a further study of the fungus and has led to the isolation of four new TDKPs including 5'-hydroxy-6'-ene-epicoccin G (1), 7-methoxy-7'-hydroxyepicoccin G (2), 8'-acetoxyepicoccin D (3), and 7'-demethoxyrostratin C (4), as well as a pair of new enantiomeric diketopiperazines (DKPs), (\pm)-5-hydroxydiphenylalazine A ((\pm)-5), together with five known analogues including diphenylalazine A (6) [4], emeheterone (7) [13], epicoccins E (8) and G (9) [4], and rostratin C (10) [7] (Figure 1). Details of the isolation and purification, structural elucidation, and cytotoxic potency against Huh7.5 liver tumor cells of compounds 1–10 are described herein.

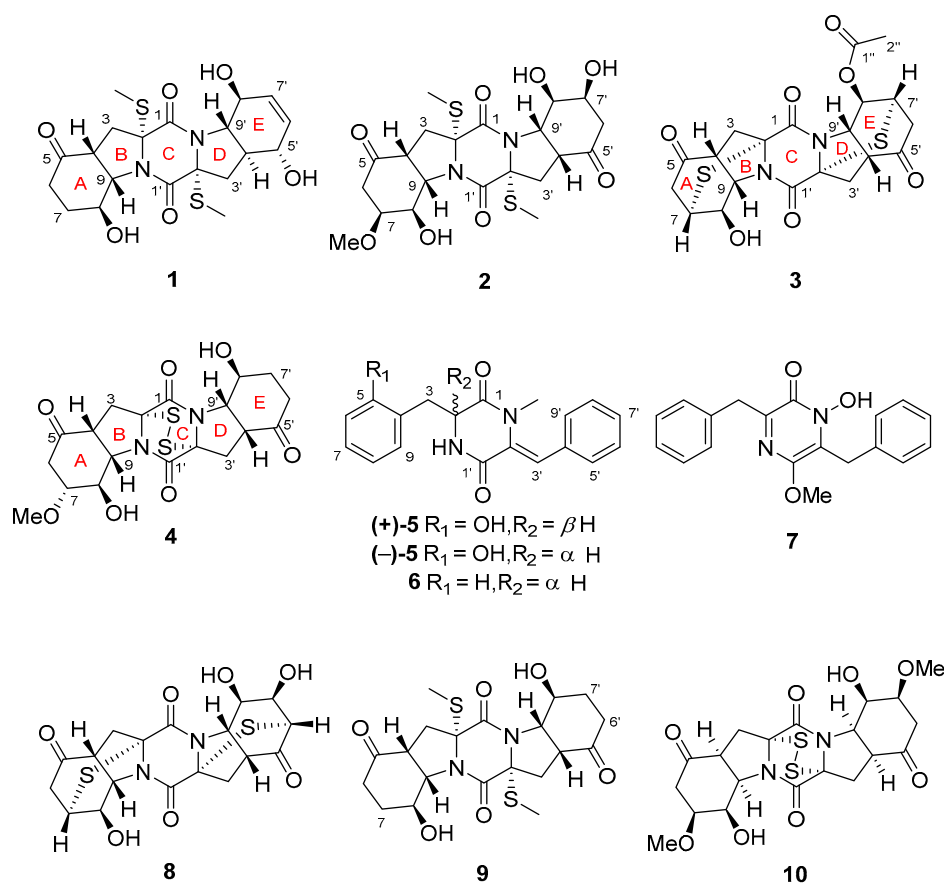


Figure 1. Structures of the isolated compounds 1–10.

2. Results and Discussion

2.1. Structure Elucidation of the New Compounds

The fungal strain *E. nigrum* SD-388 was cultured on the rice solid medium, which was further exhaustively extracted with EtOAc to afford an extract. Fractionation of the extracts by a combination of column chromatography (CC) over silica gel, Lobar LiChroprepRP-18, SephadexLH-20, as well as semi-preparative HPLC, yielded compounds 1–10.

Compound 1, initially obtained as colorless gum, gave a pseudomolecular ion peak at m/z 455.1293 $[\text{M} + \text{H}]^+$ by HR-ESI-MS, consistent with a molecular formula of $\text{C}_{20}\text{H}_{26}\text{N}_2\text{O}_6\text{S}_2$, indicating 9 degrees of unsaturation. The ^1H -, ^{13}C -NMR, and DEPT spectroscopic data (Tables 1 and 2) revealed the presence of two methyls, four sp^3 hybridized methylenes, nine methines (with five oxygenated/nitrogenated and two olefinic), five nonprotonated carbons (with one ketone and two amide carbonyls), as well as three

exchangeable protons. Detailed analysis of the NMR data disclosed that the structure of **1** was similar to that of epicoccin G (**9**), a well described TDKP derivative identified from a *Cordyceps*-colonizing fungus *Epicoccum nigrum* XZC04-CS-302 in 2009 [4]. However, signals for two CH₂ groups at $\delta_{\text{H}}/\delta_{\text{C}}$ 2.20 and 2.59/33.8 (C-6') and at $\delta_{\text{H}}/\delta_{\text{C}}$ 1.88 and 2.12/25.8 (C-7') in compound **9**, were replaced by two olefinic CH groups at $\delta_{\text{H}}/\delta_{\text{C}}$ 5.68/133.3 (C-6') and $\delta_{\text{H}}/\delta_{\text{C}}$ 5.53/129.9 (C-7') in the NMR spectra of **1**. Furthermore, the signal for the ketone group (C-5') of **9** (δ_{C} 207.7) was replaced by an oxygenated methine ($\delta_{\text{H}}/\delta_{\text{C}}$ 4.11/71.3) in **1**. The COSY correlations for the spin system from H-3' through H-9' via H-4'~H-8' and the HMBC correlations from H-5' to C-7' and C-9', from H-6' to C-4' and C-5', and from H-7' to C-9', confirmed the proposed structure of **1** (Figure 2).

Table 1. ¹H NMR spectroscopic data for compounds 1–5 ^a.

No.	1	2	3	4	5
2					4.17, t (6.4)
3	α 2.80, d (13.4)	α 2.75, d (13.5)	α 3.13, d (17.7)	α 2.68, m	a 3.02, dd (13.3, 6.4)
	β 2.28, m	β 2.35, dd (13.5, 8.5)	β 2.89, m	β 2.99, dd (14.8, 7.9)	b 2.95, dd (13.3, 6.4)
4	2.98, t (8.0)	2.92, t (8.5)	3.06, t (8.3)	3.18, t (7.9)	
6	α 2.22, m	α 2.54, dd (17.1, 4.7)	α 2.85, m	α 2.71, m	6.79, d (7.3)
	β 2.61, m	β 2.65, m	β 2.92, m	β 2.61, m	
7	α 2.19, m	3.82, ddd (10.1, 4.7, 2.0)	3.73, m	3.29, ddd (10.9, 4.7, 1.5)	6.96, m
	β 1.92, m				
8	4.36, m	4.56, m	4.01, dt (4.6, 2.4)	5.03, t (4.7)	6.67, td (7.3, 1.2)
9	4.33, m	4.33, m	4.67, dd (8.3, 2.4)	4.41, dd (7.9, 4.7)	6.98, m
3'	α 2.42, dd (12.5, 4.9)	α 2.73, d (13.4)	α 2.93, m	α 2.74, m	6.83, s
	β 2.26, m	β 2.34, dd (13.4, 8.5)	β 3.29, d (19.4)	β 2.93, dd (14.8, 8.0)	
4'	2.09, m	2.91, t (8.5)	3.17, d (8.1)	3.23, t (8.0)	
5'	4.11, m				7.27, d (7.3)
6'	5.68, d (9.8)	α 2.40, dd (16.8, 4.4)	α 2.89, m	α 2.66, m	7.40, t (7.3)
		β 2.61, m	β 2.97, m	β 2.27, dt (16.7, 4.1)	
7'	5.53, d (9.8)	4.12, ddd (10.2, 4.4, 2.0)	3.92, m	α 1.62, td (12.5, 5.0)	7.32, t (7.3)
				β 1.89, m	
8'	4.08, m	4.29, s	5.04, dd (4.3, 2.0)	4.81, m	7.40, t (7.3)
9'	3.41, dd (12.0, 8.1)	4.34, m	4.83, dd (8.1, 2.0)	4.36, m	7.27, d (7.3)
1-NMe					2.69, s
1'-NH					^b
2-SMe	1.95, s	1.93, s			
2'-SMe	2.08, s	1.92, s			
2''			2.04, s		
5-OH					8.50, br s
8-OH	5.36, d (3.2)	5.44, br s	6.25, d (2.4)	5.64, d (4.7)	
5'-OH	5.92, s				
7'-OH		5.19, br s			
8'-OH	5.28, d (5.8)	5.44, br s		5.49, d (4.0)	
7-OMe		3.25, s		3.21, s	

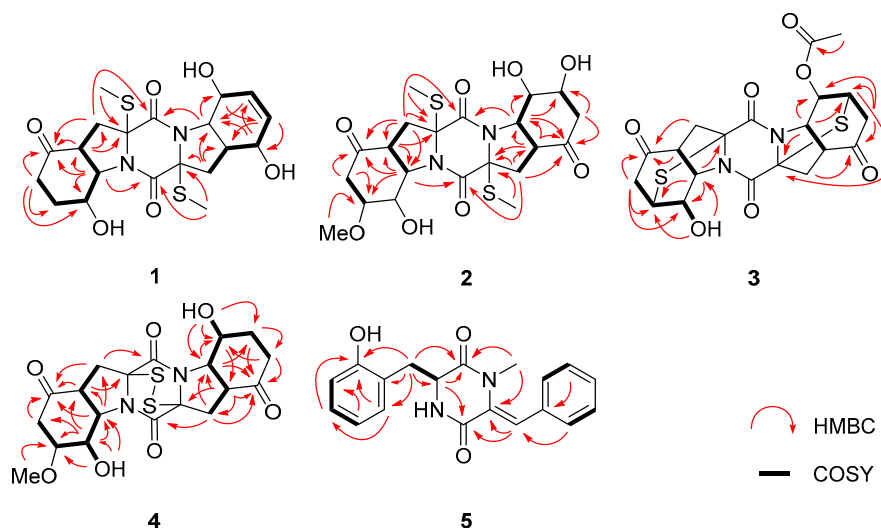
^a Data collected at 500 MHz in DMSO-*d*₆. ^b Data not detected.

The relative configuration of **1** was deduced from analysis of the NOESY spectrum. NOE correlations from H-9 to H-3 β and H-4, and from the proton of 8-OH to H-4, H-6 β , and H-7 β , indicated the cofacial orientation of these groups (Figure 3). Besides, NOEs from H-3 α to 2-SMe placed them on another face, opposite to that of H-4, H-9, and 8-OH. Moreover, NOE cross-peaks from H-8' to H-3' α and H-4', and from H-3' α to 2'-SMe, confirmed them on the same spatial orientation, while NOE correlations from H-5' to H-9' and H-3' β placed these groups on the opposite face. On the basis of the above observation, the relative configurations for rings A/B and D/E were determined respectively. However, the relationship between these two units could not be correlated based on the NOESY experiment, because no diagnostic NOE cross-peak could be detected between rings A/B and D/E.

Table 2. ^{13}C NMR spectroscopic data for compounds 1–5 ^a.

No.	1	2	3	4	5
1	168.7, C	165.5, C	158.3, C	162.2, C	167.2, C
2	71.4, C	71.6, C	71.1, C	76.2, C	55.6, CH
3	34.3, CH ₂	34.4, CH ₂	41.4, CH ₂	32.6, CH ₂	34.8, CH ₂
4	44.0, CH	43.8, CH	45.0, CH	46.4, CH	122.0, C
5	207.5, C	206.6, C	207.1, C	207.8, C	156.1, C
6	33.8, CH ₂	40.4, CH ₂	43.2, CH ₂	40.7, CH ₂	115.1, CH
7	25.9, CH ₂	75.8, CH	41.3, CH	75.5, CH	127.8, CH
8	63.6, CH	61.5, CH ^b	65.2, CH	61.9, CH	118.4, CH
9	64.8, CH	63.2, CH	60.3, CH	63.2, CH	131.2, CH
1'	165.5, C	165.4, C	158.9, C	162.2, C	162.4, C
2'	72.9, C	71.6, C	71.7, C	76.4, C	132.2, C
3'	35.1, CH ₂	34.1, CH ₂	41.5, CH ₂	32.2, CH ₂	117.7, CH
4'	43.4, CH	43.5, CH	45.3, CH	46.7, CH	133.8, C
5'	71.3, CH	207.4, C	206.3, C	208.6, C	129.4, CH
6'	133.3, CH	43.3, CH ₂	43.5, CH ₂	33.9, CH ₂	128.1, CH
7'	129.9, CH	65.7, CH	38.8, CH	25.4, CH ₂	127.9, CH
8'	68.9, CH	68.1, CH ^b	67.4, CH	60.8, CH	128.1, CH
9'	67.8, CH	62.7, CH	57.5, CH	65.8, CH	129.4, CH
1''			168.8, C		
2''			20.6, CH ₃		
1-NMe					34.5, CH ₃
2-SMe	14.4, CH ₃	14.2, CH ₃			
2'-SMe	14.2, CH ₃	13.9, CH ₃			
7-OMe		55.8, CH ₃		56.0, CH ₃	

^a Data collected at 125 MHz in DMSO-*d*₆. ^b Assigned by HSQC experiment.

**Figure 2.** Key ^1H - ^1H COSY (bold lines) and HMBC (red arrows) correlations of compounds 1–5.

To fully assign the configuration of compound **1**, efforts toward a single crystal X-ray study were performed. By slow evaporation of the solvent (MeOH–H₂O, 100:1) under refrigeration, quality crystals of **1** were obtained, making it feasible for an X-ray crystallographic experiment which confirmed not only the planar structure, but also the relative configuration of compound **1** (Figure 4). The defined Flack parameter 0.01(3) determined the absolute configuration of **1** as *2R, 4R, 8S, 9S, 2'R, 4'S, 5'S, 8'S*, and *9'S*, and the trivial name 5'-hydroxy-6'-ene-epicoccin G was assigned to compound **1**.

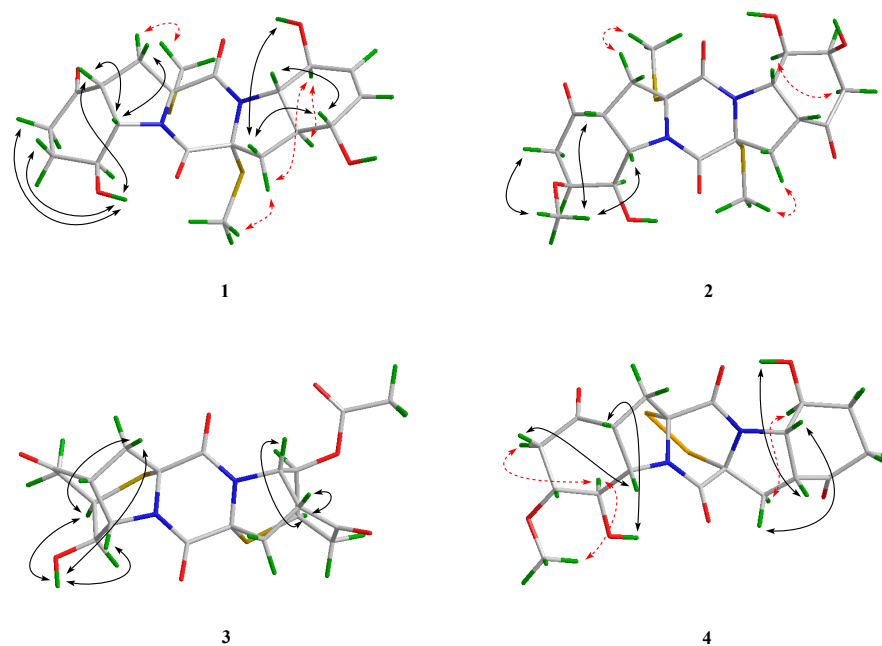


Figure 3. Key NOE correlations of compounds 1–4 (black solid lines: β -orientation; red dashed lines: α -orientation).

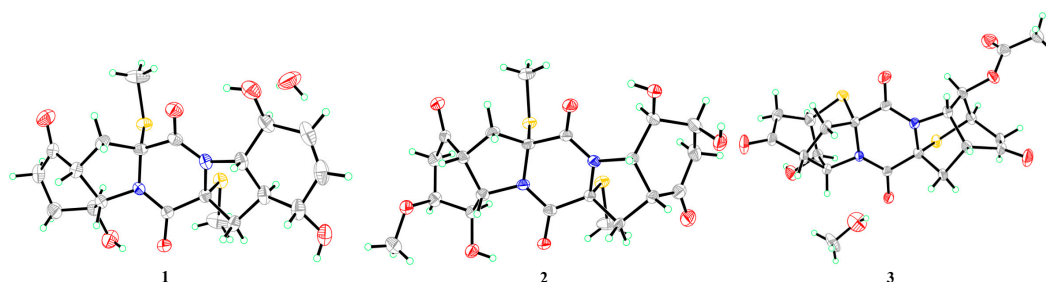


Figure 4. X-ray crystallographic structures of compounds 1–3.

The elemental composition of **2** was established to be $C_{21}H_{28}N_2O_8S_2$ by analysis of HR-ESI-MS and NMR data, indicating nine degrees of unsaturation. The 1H - and ^{13}C -NMR data of **2** were similar to those of epicoccin G (**9**), a symmetrical TDKP derivative characterized from *E. nigrum* XZC04-CS-302 [4], except that the signals of two methylene groups at δ_H/δ_C 1.88 and 2.12/25.8 (CH_2 -7 and CH_2 -7') in **9** were replaced by two oxygenated methine groups at δ_H/δ_C 3.82/75.8 (CH -7) and δ_H/δ_C 4.12/65.7 (CH -7') in **2**, respectively. Moreover, signals for a methoxy group at δ_H/δ_C 3.25/55.8 (7-OMe) were also observed (Tables 1 and 2). The methoxy group was assigned at C-7 based on the observed HMBC correlation from 7-OMe to C-7. Supported by key COSY correlations from H-6 to H-7, and from H-6' to H-7', as well as by HMBC correlations from H-6 and H-9 to C-7 and from H-6' and H-9' to C-7' (Figure 2), the planar structure of compound **2** was determined.

The relative configuration of **2** was assigned by analysis of J -coupling constants and NOESY data. A coupling constant of 8.5 Hz between H-4 and H-9 as well as between H-4' and H-9' suggested their *cis* relationships, as reported in the previous literature [7]. NOE correlations from the proton of 7-OMe to H-4 and H-9 indicated the cofacial orientation of these groups. However, the relative configurations of **2** could not be fully assigned due to the lack of some key NOE correlations.

A single crystal of **2** was cultivated, after attempts by dissolving the samples in MeOH–H₂O (100:1) followed by slow evaporation under refrigeration for two weeks. Once the Cu/K α X-ray crystallographic experiment was conducted (Figure 4), the structure and absolute configuration of

2 were assigned as *2R, 4R, 7S, 8R, 9S, 2'R, 4'R, 7'S, 8'R, and 9'S*, with a Flack parameter of 0.02(4). Compound **2** was named 7-methoxy-7'-hydroxyepicoccin G.

The accurate mass data measured by HR-ESI-MS of compound **3** assigned its molecular formula, $C_{20}H_{20}N_2O_7S_2$ (12 degrees of unsaturation), and was supported by the NMR data. The 1H - and ^{13}C -NMR data of **3** (Tables 1 and 2) showed close similarity to those of epicoccin D, a TDKP derivative isolated from the fungal strain *E. nigrum* (2203) in 2007 [3]. However, resonances for an ester carbonyl carbon (δ_C 168.8, C-1'') and a methyl group (δ_H/δ_C 2.04/20.6, CH₃-2'') were observed in the NMR spectra of **3**. Deshielded shift at δ_H 5.04 for H-8' in **3** was detected, compared to that of δ_H 4.00 in epicoccin D. The above observation suggested that compound **3** was a C-8' acetylated derivative of epicoccin D. The relative configuration of **3** was assigned on the basis of the NOESY experiment and *J*-coupling constants. For ring A of **3**, NOE correlations from the proton of OH-8 to H-7 and H-9 revealed the same orientation of these groups (Figure 3). In addition, the *cis* relationship between H-4 and H-9 was established by the coupling constant (*J* = 8.3 Hz) which is in agreement with that of rostratin B (*J* = 7.2 Hz) [7]. However, the relative configurations of ring E could not be solved as it lacked some key NOE correlations. To unequivocally determine the relative and absolute configurations, single crystals for **3** were cultivated upon slow evaporation of the solvent (MeOH) and a Cu/K α X-ray diffraction analysis was conducted (Figure 4). The final refinement of the X-ray data resulted in a 0.02(3) Flack parameter, allowing for the assignment of the absolute configuration as *2R, 4R, 7R, 8R, 9S, 2'R, 4'R, 7'R, 8'R, and 9'S*.

Compound **4** was initially isolated as a colorless powder. Its molecular formula was postulated as $C_{19}H_{22}N_2O_7S_2$ through HR-ESI-MS analysis, indicating 10 degrees of unsaturation. The 1D NMR data of **4** were similar to those of rostratin C (**10**), a DKP derivative isolated from the marine-derived fungal strain *Exserohilum rostratum* CNK-630 [7], with the exception of the disappeared signals for the oxygenated methine (C-7') and the methoxy group attached to C-7'. In contrast, signals for a methylene group at δ_H 1.62/1.89 and δ_C 25.4 (CH₂-7') were observed in the NMR spectra of **4** (Tables 1 and 2), indicating that **4** is a 7'-demethoxy derivative of **10**. The 2D NMR correlations supported this inference by the COSY correlations from H-7' to H-6' and H-8', and HMBC correlations from H-7' to C-5' and from H-9' to C-7' (Figure 2).

The relative configuration for rings A and E of **4** were determined by analysis of NOESY data. NOE correlations, with respect to ring A from H-8 to H-3 α and 7-OMe, placed them on the same face. Meanwhile, NOEs from the proton of 8-OH to H-4, and from H-3 β to H-9, disclosed the cofacial orientation of these groups. As for ring E, the coupling constant (*J* = 8.0 Hz) observed between H-4' and H-9' revealed their *cis* relationship [7]. In addition, NOEs from the proton of 8'-OH to H-4', and from H-3' β to H-9', revealed them on the cofacial orientation. Whereas NOE from H-3' α to H-8' revealed that these groups were on the other face (Figure 3).

The assignment of the absolute configurations at C-2/C-2' were established by analysis of ECD cotton effects (CEs) following the rules reported by the previous reference [14]. The ECD spectrum of **4** showed a positive CE near 265 nm, which was characteristic for the *2R/2'R* configurations in TDKPs. The whole absolute configuration of **4** was further studied using the time-dependent density functional (TDDFT)-ECD calculation in Gaussian 09. The ECD spectra of four possible stereoisomers of **4**, including (*2R, 4R, 7R, 8R, 9S, 2'R, 4'R, 8'S, 9'S*)-**4**, (*2R, 4R, 7R, 8R, 9S, 2'R, 4'S, 8'R, 9'R*)-**4**, (*2R, 4S, 7S, 8S, 9R, 2'R, 4'R, 8'S, 9'S*)-**4**, and (*2R, 4S, 7S, 8S, 9R, 2'R, 4'S, 8'R, 9'R*)-**4**, were calculated. The experimental ECD spectrum for **4** showed agreement with that calculated for (*2R, 4R, 7R, 8R, 9S, 2'R, 4'R, 8'S, 9'S*)-**4** (Figure 5a), allowing the elucidation of whole chiral centers as *2R, 4R, 7R, 8R, 9S, 2'R, 4'R, 8'S, and 9'S*.

Compound **5**, obtained as a yellow oil, was assigned the molecular formula $C_{19}H_{18}N_2O_3$ by HR-ESI-MS, and required 12 degrees of unsaturation. Analysis of the 1H - and ^{13}C -NMR data (Tables 1 and 2) revealed that compound **5** had same basic structure as that of the previously reported diphenylalazine A (**6**), which was identified from the fungus *E. nigrum* XZC04-CS-302 [4]. However, the aromatic methine at C-5 in **6** (δ_H/δ_C 7.18/129.82) was replaced by a nonprotonated and hydroxylated

carbon (δ_C 156.1) in **5**. HMBC correlations from H-3, H-7, and H-9 to C-5, supported this deduction. The planar structure of **5** was thus established as 5-hydroxydiphenylazazine A. However, the specific optical rotation value of $[\alpha]_{25}^D = 0$ (c 0.10, MeOH) revealed the racemic nature of compound **5**, which was also confirmed by the fact that no cotton effects were observed in the ECD spectrum (Figure S36). Separation of **5** by HPLC using the Daicel Chiral-pak IC column yielded (+)-**5** and (–)-**5** (Figure S37), which were individually determined absolute configurations by experimental and calculated ECD spectra (Figure 5b), and assigned (+)-**5** as 2*R* and (–)-**5** as 2*S*.

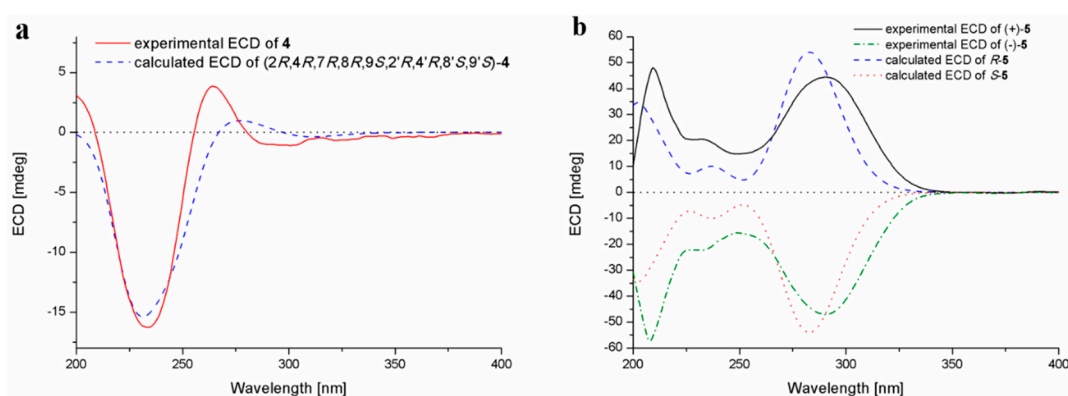


Figure 5. Experimental and calculated ECD spectra of compounds **4** (a) and **5** (b).

In addition to compounds **1–5**, five known analogues (**6–10**) were also isolated. By detailed spectroscopic analysis as well as comparison with reported data, the structures of compounds **6–10** were identified as diphenylazazines A (**6**) [4], emeheterone (**7**) [13], epicoccins E (**8**) and G (**9**) [4], and rostratin C (**10**) [7].

2.2. Biological Activities of the Isolated Compounds

All of the isolated compounds were assayed for their activities against Huh7.5 liver tumor cells. Among them, only compounds **4** and **10** displayed significant cytotoxic effects against Huh7.5 with cell viability less than 30% at the concentration of 20 μ M. As shown in Figure 6, the growth-inhibiting effects of **4** and **10** were concentration-dependent, with IC_{50} values of 9.52 and 4.88 μ M, respectively, which were comparable to that of the positive control, sorafenib (IC_{50} 8.2 μ M). Compounds **4** and **10** were also measured for their cytotoxicity against human normal liver LO2 cell line. The results showed that compound **4** exhibited the inhibitory effects against normal liver cells, similar to that of cancer cells (Figure 6). However, compound **10** was less sensitive to normal liver cells than liver cancer cells, only at a narrow concentration range of 4–10 μ M. The results suggested that the disulfide bridge at C-2/C-2' is likely essential for the activity.

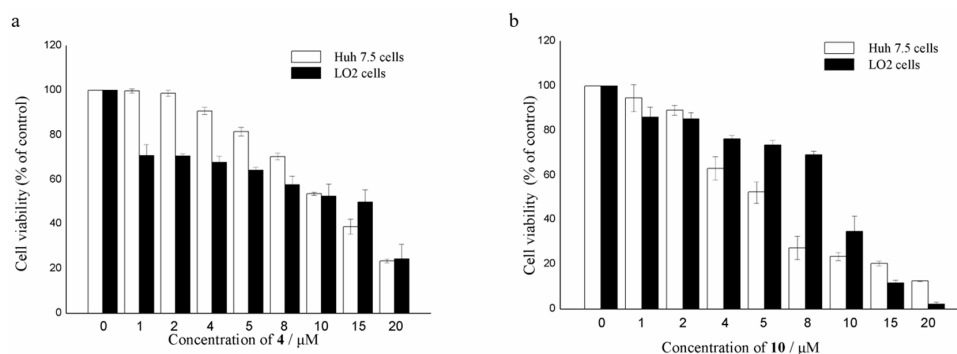


Figure 6. Cell viability of Huh7.5 liver cancer cells and LO2 normal liver cells treated with compounds **4** (a) and **10** (b).

3. Experimental Section

3.1. General Experimental Procedures

Melting points were acquired through an SGW X-4 micro-melting-point apparatus (Shanghai Shengguang Instrument Co. Ltd, Shanghai, China). Optical rotations were measured using an Optical Activity AA-55 polarimeter (Optical Activity Ltd., Cambridgeshire, UK). UV spectra were determined by a PuXi TU-1810 UV-visible spectrophotometer (Shanghai Lengguang Technology Co. Ltd., Shanghai, China), and ECD spectra were obtained with a JASCO J-715 spectropolarimeter (JASCO, Tokyo, Japan). NMR spectra were recorded on a Bruker Avance 500 spectrometer (Bruker Biospin Group, Karlsruhe, Germany), using solvent chemical shifts (DMSO- d_6 : δ_H/δ_C 2.50/39.52) as reference. HR-ESI-MS were measured on an API QSTAR Pulsar 1 mass spectrometer (Applied Biosystems, Foster, Waltham, MA, USA). Analytical and semi-preparative reversed-phase HPLC separations were performed by a Dionex HPLC system, equipped with P680 pump (Dionex, Sunnyvale, CA, USA), ASI-100 automated sample injector, and UVD340U multiple wavelength detector controlled by Chromeleon software (version 6.80). Commercially available Lobar LiChroprep RP-18 (40–63 μm , Merck, Darmstadt, Germany), Si gel (200–300 mesh, Qingdao Haiyang Chemical Co., Qingdao, China), and Sephadex LH-20 (Pharmacia, Pittsburgh, PA, USA) were used for column chromatography. Thin-layer chromatography (TLC) was carried out using precoated Si gel GF₂₅₄ plates (Merck, Darmstadt, Germany). All solvents used were distilled prior to use.

3.2. Fungal Material

The fungal strain *Epicoccum nigrum* SD-388 was isolated from the deep-sea sediment collected in the West Pacific (depth 4500 m) on March 2015. The fungus was identified using a molecular biological protocol by DNA amplification and sequencing of the ITS (internal transcript spacer) region. The sequence data for the fungus have been deposited in GenBank with the accession no. MN089646. Through the BLAST searching, the fungus was identified as *Epicoccum nigrum* according to the ITS region sequence, which is the same (100%) as that of *E. nigrum* (accession no. KU254609). The strain is preserved at the Key Laboratory of Experimental Marine Biology, Institute of Oceanology, Chinese Academy of Sciences (IOCAS).

3.3. Fermentation

For chemical investigations, the fresh mycelia of the fungus were grown on PDA medium at 28 °C for one week and were then inoculated into 1 L Erlenmeyer flasks. The fungus was fermented statically at room temperature for 35 days in rice solid medium containing rice (70 g/flask), peptone (0.3%), yeast extract (0.5%), corn steep liquor (0.2%), monosodium glutamate (0.1%), Fe₂(SO₄)₃ (0.002%), MgSO₄·7H₂O (0.07%), ZnSO₄ (0.0001%), KH₂PO₄ (0.025%), and naturally sourced and filtered seawater (obtained from the Huiquan Gulf of the Yellow Sea near the campus of IOCAS, 100 mL/flask).

3.4. Extraction and Isolation

The fermented rice substrate was mechanically fragmented after incubation, and then extracted with petroleum ether (PE) to remove the low-polarity chemical constituents. The remaining culture was extracted thoroughly with EtOAc, which was filtered and evaporated under reduced pressure to give EtOAc extract (75.5 g).

The EtOAc extract was fractionated by Si gel VLC (vacuum liquid chromatography), using solvents of increasing polarity (PE-EtOAc, 20:1 to 1:1, and then CH₂Cl₂-MeOH, 20:1 to 1:1) to yield nine fractions (Frs. 1–9). Fr. 5 (6.6 g) was further separated by CC (Column Chromatography) over Lobar LiChroprep RP-18 with a MeOH-H₂O gradient (from 1:9 to 10:0) to yield 10 subfractions (Frs. 5.1–5.10). Fr. 5.4 (453.8 mg) was subjected to CC on Si gel eluting with a CH₂Cl₂-MeOH gradient (from 500:1 to 200:1) to yield compounds 6 (187.6 mg) and 7 (15.5 mg). Fr. 6 (29.2 g) was repeatedly subjected to Si gel VLC and then fractionated by solvents of increasing polarity from CH₂Cl₂ to acetone to yield

four subfractions (Fr. 6.1–6.4) based on HPLC and TLC analysis. Purification of Fr. 6.1 (6.2 g) by CC over Lobar LiChroprep RP-18 with a MeOH-H₂O gradient (from 1:9 to 10:0) yielded 10 subfractions (Fr. 6.1.1–6.1.10). Fr. 6.1.1 (14.3 mg) was recrystallized from mixed solvents (MeOH-H₂O, 10:1) to give **3** (6.7 mg). Fr. 6.1.2 (53.7 mg) was purified by prep-TLC and CC on Sephadex LH-20 (MeOH) to obtain **10** (34.1 mg). Fr. 6.1.3 (44.8 mg) was also recrystallized from MeOH to give **9** (21.9 mg). Fr. 6.1.4 (79.2 mg) was applied to semi-preparative HPLC (Elite ODS-BP column, 10 μm; 20 × 250 mm; 70% MeOH-H₂O, 16 mL/min) to afford **4** (18.3 mg, *t_R* 29.6 min). Fr. 6.1.5 (207.3 mg) was subjected to repeated CC on silica gel (CH₂Cl₂-MeOH, 140:1) and purified by prep-TLC and CC on Sephadex LH-20 (MeOH) to give **5** (9.4 mg). Fr. 6.2 (6.0 g) was split by CC over Lobar LiChroprep RP-18, silica gel, and Sephadex LH-20 to yield **2** (12.5 mg). Fr. 6.3 (6.5 g) was subjected to CC over Lobar LiChroprep RP-18, eluted with a MeOH-H₂O gradient (from 1:9 to 10:0) to yield 10 subfractions (Fr. 6.3.1–6.3.10). Fr. 6.3.1 (32.1 mg) was recrystallized from mixed solvents (MeOH-H₂O, 10:1) to afford **8** (13.7 mg). Fr. 6.3.3 (108.9 mg) was purified by semi-preparative HPLC (Elite ODS-BP column, 10 μm; 20 × 250 mm; 72% MeOH-H₂O, 16 mL/min) to afford **1** (46.8 mg, *t_R* 31.2 min).

5'-Hydroxy-6'-ene-epicoccin G (**1**): Colorless cube crystal (MeOH-H₂O); mp 161–163 °C; $[\alpha]_{25}^D$ −95.7 (*c* 0.23, MeOH); UV (MeOH) λ_{\max} (log ϵ) 204 (3.99) nm; ECD (4.18 mM, MeOH) λ_{\max} ($\Delta\epsilon$) 200 (−1.96), 233 (+2.46), 260 (−3.07) nm; ¹H and ¹³C NMR data, Tables 1 and 2; ESIMS *m/z* 455 [M + H]⁺; HRESIMS *m/z* 455.1293 [M + H]⁺ (calcd for C₂₀H₂₇O₆N₂S₂, 455.1305).

7-Methoxy-7'-hydroxyepicoccin G (**2**): Colorless cube crystal (MeOH); mp 173–175 °C; $[\alpha]_{25}^D$ −138.9 (*c* 0.18, MeOH); UV (MeOH) λ_{\max} (log ϵ) 204 (4.16) nm; ECD (4.80 mM, MeOH) λ_{\max} ($\Delta\epsilon$) 200 (−3.35), 231 (+3.91), 259 (−2.53) nm; ¹H and ¹³C NMR data, Tables 1 and 2; ESIMS *m/z* 501 [M + H]⁺; HRESIMS *m/z* 501.1360 [M + H]⁺ (calcd for C₂₁H₂₉O₈N₂S₂, 501.1360).

8'-Acetoxyepicoccin D (**3**): Colorless needle crystal (MeOH); mp 233–235 °C; $[\alpha]_{25}^D$ +225.6 (*c* 0.02, MeOH); UV (MeOH) λ_{\max} (log ϵ) 204 (3.75) nm; ECD (2.15 mM, MeOH) λ_{\max} ($\Delta\epsilon$) 218 (+1.24), 252 (+0.31), 290 (−0.10) nm; ¹H and ¹³C NMR data, Tables 1 and 2; ESIMS *m/z* 482 [M + NH₄]⁺, *m/z* 487 [M + Na]⁺; HRESIMS *m/z* 482.1045 [M + NH₄]⁺ (calcd for C₂₀H₂₄O₇N₃S₂, 482.1050), 487.0601 [M + Na]⁺ (calcd for C₂₀H₂₀O₇N₂NaS₂, 487.0604).

7'-Demethoxyrostratin C (**4**): Colorless amorphous powder; $[\alpha]_{25}^D$ −215.4 (*c* 0.13, MeOH); UV (MeOH) λ_{\max} (log ϵ) 201 (4.06) nm; ECD (2.20 mM, MeOH) λ_{\max} ($\Delta\epsilon$) 200 (+0.43), 234 (−2.24), 265 (+0.53) nm; ¹H and ¹³C NMR data, Tables 1 and 2; ESIMS *m/z* 455 [M + H]⁺; HRESIMS *m/z* 455.0930 [M + H]⁺ (calcd for C₁₉H₂₃O₇N₂S₂, 455.0941).

(±)-5-Hydroxydiphenylalazine A (**5**): Yellow oil; UV (MeOH) λ_{\max} (log ϵ) 200 (4.49) nm, 216 (4.19) nm, 283 (4.14) nm; ¹H and ¹³C NMR data, Tables 1 and 2; ESIMS *m/z* 323 [M + H]⁺; HRESIMS *m/z* 323.1383 [M + H]⁺ (calcd for C₁₉H₁₉O₃N₂, 323.1390).

(+)-**5**: $[\alpha]_{25}^D$ +350 (*c* 0.18, MeOH); ECD (5.59 mM, MeOH) λ_{\max} ($\Delta\epsilon$) 209 (+2.59), 233 (+1.11), 291 (+2.41) nm.

(−)-**5**: $[\alpha]_{25}^D$ −345 (*c* 0.18, MeOH); ECD (5.59 mM, MeOH) λ_{\max} ($\Delta\epsilon$) 206 (−3.11), 242 (−1.21), 288 (−2.55) nm.

3.5. X-Ray Crystallographic Analysis

Crystallographic data have been deposited in the Cambridge Crystallographic Data Centre [15]. Crystallographic data were collected on an Agilent Xcalibur Eos Gemini CCD plate diffractometer equipped with a graphite-monochromatic Cu-K α radiation (λ = 1.54178) Å at 293 (2) K. The data were corrected for absorption by using the program SADABS [16]. The structures were solved by

direct methods with the SHELXTL software package [17]. All non-hydrogen atoms were refined anisotropically. The H atoms connected to C atoms were calculated theoretically, and those to O atoms were assigned by difference Fourier maps [18]. The absolute structure was determined by refinement of the Flack parameter [19], based on anomalous scattering. The structures were optimized by full-matrix least-squares techniques.

Crystal data of compound 1: $C_{20}H_{26}N_2O_6S_2 \cdot H_2O$, F.W. = 472.56, orthorhombic space group $P2(1)2(1)2(1)$, unit cell dimensions $a = 8.5746$ (5) Å, $b = 10.9602$ (8) Å, $c = 24.3158$ (16) Å, $V = 2285.2$ (3) Å³, $\alpha = \beta = \gamma = 90^\circ$, $Z = 4$, $d_{\text{calcd}} = 1.374$ mg/m³, crystal dimensions $0.40 \times 0.21 \times 0.13$ mm, $\mu = 2.491$ mm⁻¹, $F(000) = 1000$. The 5006 measurements yielded 3321 independent reflections after equivalent data were averaged. The final refinement gave $R_1 = 0.0525$ and $wR_2 = 0.1263$ [$I > 2\sigma(I)$]. The absolute structure parameter was 0.01(3).

Crystal data of compound 2: $C_{21}H_{28}N_2O_8S_2$, F.W. = 500.57, monoclinic space group $P2(1)$, unit cell dimensions $a = 6.8423$ (4) Å, $b = 20.5136$ (10) Å, $c = 8.2231$ (5) Å, $V = 1130.48$ (11) Å³, $\alpha = \gamma = 90^\circ$, $\beta = 101.635$ (2)°, $Z = 2$, $d_{\text{calcd}} = 1.471$ mg/m³, crystal dimensions $0.20 \times 0.17 \times 0.10$ mm, $\mu = 2.587$ mm⁻¹, $F(000) = 528$. The 6832 measurements yielded 2789 independent reflections after equivalent data were averaged. The final refinement gave $R_1 = 0.0514$ and $wR_2 = 0.1199$ [$I > 2\sigma(I)$]. The absolute structure parameter was 0.02(4).

Crystal data of compound 3: $C_{20}H_{20}N_2O_7S_2 \cdot CH_3OH$, F.W. = 496.54, orthorhombic space group $P2(1)2(1)2(1)$, unit cell dimensions $a = 10.1030$ (6) Å, $b = 10.8478$ (5) Å, $c = 19.6848$ (10) Å, $V = 2157.4$ (2) Å³, $\alpha = \beta = \gamma = 90^\circ$, $Z = 4$, $d_{\text{calcd}} = 1.529$ mg/m³, crystal dimensions $0.25 \times 0.17 \times 0.13$ mm, $\mu = 2.711$ mm⁻¹, $F(000) = 1040$. The 4782 measurements yielded 3033 independent reflections after equivalent data were averaged. The final refinement gave $R_1 = 0.0510$ and $wR_2 = 0.1001$ [$I > 2\sigma(I)$]. The absolute structure parameter was 0.02(3).

3.6. Computational Section

Conformational searches were carried out via molecular mechanics with the MM+ method in HyperChem 8.0 software (Gainesville, FL, USA). Afterwards, the geometries were optimized at the gas-phase B3LYP/6-31G level in Gaussian09 software to afford the energy-minimized conformers. Then, the optimized conformers were subjected to the calculations of ECD spectra using the TD-DFT at BH&HLYP/TZVP level for 4 and PBE0/TZVP level for 5. Simultaneously, solvent effects of the MeOH solution were evaluated at the same DFT level using the SCRF/PCM method [20].

3.7. Cytotoxic Assays

3.7.1. Cell Culture

Liver cancer Huh7.5 cell line used was obtained from the American Type Culture Collection (ATCC). Human normal liver LO2 cell line used was purchased from China Center for Type Culture Collection (CCTCC). Huh7.5 cells and LO2 cells were cultured at 37 °C in RPMI-1640 medium and DMEM medium, respectively, supplemented with 10% fetal bovine serum (FBS, PAN Biotech, Aidenbach, Germany), 100 U/mL penicillin, and 100 mg/mL streptomycin. All experiments were carried out with the same batch of cell line between passages 2 and 5 [21].

3.7.2. Cell Proliferation Assay

The cytotoxic activities of compounds 1–10 against Huh7.5 liver tumor cells and human normal liver LO2 cell line were determined by the 3-(4,5-dimethylthiazolyl-2)-2,5-diphenyltetrazolium bromide (MTT) assay. Briefly, 6×10^3 of logarithmically growing Huh7.5 cells and human normal liver LO2 cell line were plated in the 96-well plate at 37 °C for 24 h. Then, cells were treated with DMSO (as the vehicle control) and increasing concentrations of test compounds (with the final concentration of 1, 2, 4, 5, 8, 10, 15, 20 µM) for 48 h, respectively. MTT solution (5 mg/mL, 20 µL per well) was added and incubated for another 4 h. After supernate from the wells were removed, DMSO was added to

each well to dissolve purple crystals of formazan with gentle shaking for 10 min, and optical density at 490 nm was read by a multi-detection microplate reader (Infinite M1000 Pro, Tecan, Switzerland). Sorafenib was used as positive control. All the compounds and positive control were dissolved and diluted in DMSO. All tests were performed in triplicate. The values of relative cell viability were calculated as percentages of absorbance from the treated samples to absorbance from the vehicle control [21].

4. Conclusions

In conclusion, ten diketopiperazine alkaloids including four new derivatives, 5'-hydroxy-6'-ene-epicoccin G (1), 7-methoxy-7'-hydroxyepicoccin G (2), 8'-acetoxyepicoccin D (3), and 7'-demethoxyrostratin C (4), and a pair of new enantiomeric diketopiperazines (\pm)-5-hydroxydiphenylalazine A (\pm)-5), along with five known analogues (6–10) were characterized from the deep sea-derived fungus *E. nigrum* SD-388. The discovery of these compounds might provide further insight into the biosynthesis of the diketopiperazine family and provide new targets for synthetic or biosynthetic studies. Compounds 4 and 10 exhibited potent cytotoxic activities against Huh7.5 liver cancer cells and may provide useful candidates for further study as antitumor agents.

Supplementary Materials: Selected 1D and 2D NMR, HRESIMS, and ECD spectra of compounds 1–5 are available online at: <http://www.mdpi.com/1660-3397/18/3/160/s1>.

Author Contributions: L.-P.C. performed the experiments for the isolation, structure elucidation, and prepared the manuscript; X.-M.L. performed the 1D and 2D NMR experiments; L.L. participated in the isolation of the fungus *Epicoccum nigrum*. X.L. contributed to ECD calculations and revised the manuscript; B.-G.W. All authors have read and agreed to the published version of the manuscript.

Funding: This research work was financially supported by the Strategic Priority Research Program of the Chinese Academy of Sciences (XDA22050401) and the Aoshan Scientific and Technological Innovation Project of Qingdao National Laboratory for Marine Science and Technology (2016ASKJ14). X.L. appreciates the China Postdoctoral Science Foundation (2017M612360) for project funding. B.-G.W. acknowledges the support of the Research Vessel KEXUE of the National Major Science and Technology Infrastructure from the Chinese Academy of Sciences (KEXUE2018G28) and the Taishan Scholar Project from Shandong Province.

Acknowledgments: The authors appreciate Chao-min Sun and Ge Liu at the Institute of Oceanology, Chinese Academy of Sciences, for their support in cytotoxic assays, and the High Performance Computing Environment Qingdao Branch of the Chinese Academy of Science (CAS)–High Performance Computing Center of Institute of Oceanology of CAS for CPU time.

Conflicts of Interest: The authors declare no conflicts of interest.

References

1. Niu, S.; Xia, M.; Chen, M.; Liu, X.; Li, Z.; Xie, Y.; Shao, Z.; Zhang, G. Cytotoxic polyketides isolated from the deep-sea-derived fungus *Penicillium chrysogenum* MCCC 3A00292. *Mar. Drugs* **2019**, *17*, 686. [[CrossRef](#)] [[PubMed](#)]
2. Liu, Z.; Fan, Z.; Sun, Z.; Liu, H.; Zhang, W. Dechdigliotoxins A–C, three novel disulfide-bridged gliotoxin dimers from deep-sea sediment derived fungus *Dichotomomyces cejpaii*. *Mar. Drugs* **2019**, *17*, 596. [[CrossRef](#)] [[PubMed](#)]
3. Zhang, Y.; Liu, S.; Che, Y.; Liu, X. Epicoccins A–D, epipolythiodioxopiperazines from a *Cordyceps*-colonizing isolate of *Epicoccum nigrum*. *J. Nat. Prod.* **2007**, *70*, 1522–1525. [[CrossRef](#)] [[PubMed](#)]
4. Guo, H.; Sun, B.; Gao, H.; Chen, X.; Liu, S.; Yao, X.; Liu, X.; Che, Y. Diketopiperazines from the *Cordyceps*-colonizing fungus *Epicoccum nigrum*. *J. Nat. Prod.* **2009**, *72*, 2115–2119. [[CrossRef](#)] [[PubMed](#)]
5. Yan, Z.; Wen, S.; Ding, M.; Guo, H.; Huang, C.; Zhu, X.; Huang, J.; She, Z.; Long, Y. The purification, characterization, and biological activity of new polyketides from mangrove-derived endophytic fungus *Epicoccum nigrum* SCNU-F0002. *Mar. Drugs* **2019**, *17*, 414. [[CrossRef](#)] [[PubMed](#)]
6. Sun, H.H.; Mao, W.J.; Jiao, J.Y.; Xu, J.C.; Li, H.Y.; Chen, Y.; Xu, J.; Zhao, C.Q.; Hou, Y.J.; Yang, Y.P. Structural characterization of extracellular polysaccharides produced by the marine fungus *Epicoccum nigrum* JJY-40 and their antioxidant activities. *Mar. Biotechnol.* **2011**, *13*, 1048–1055. [[CrossRef](#)] [[PubMed](#)]

7. Tan, R.X.; Jensen, P.R.; Williams, P.G.; Fenical, W. Isolation and structure assignments of rostratins A–D, cytotoxic disulfides produced by the marine-derived fungus *Exserohilum rostratum*. *J. Nat. Prod.* **2004**, *67*, 1374–1382. [CrossRef] [PubMed]
8. Meng, L.H.; Li, X.M.; Lv, C.T.; Huang, C.G.; Wang, B.G. Brocazines A–F, cytotoxic bithiodiketopiperazine derivatives from *Penicillium brocae* MA-231, an endophytic fungus derived from the marine mangrove plant *Avicennia marina*. *J. Nat. Prod.* **2014**, *77*, 1921–1927. [CrossRef] [PubMed]
9. Liu, Y.; Li, X.M.; Meng, L.H.; Jiang, W.L.; Xu, G.M.; Huang, C.G.; Wang, B.G. Bithiodiketopiperazines and acorane sesquiterpenes produced by the marine-derived fungus *Penicillium adametzioides* AS-53 on different culture media. *J. Nat. Prod.* **2015**, *78*, 1294–1299. [CrossRef] [PubMed]
10. Cao, J.; Li, X.M.; Meng, L.H.; Konuklugil, B.; Li, X.; Li, H.L.; Wang, B.G. Isolation and characterization of three pairs of indolediketopiperazine enantiomers containing infrequent *N*-methoxy substitution from the marine algal-derived endophytic fungus *Acrostalagmus luteoalbus* TK-43. *Bioorg. Chem.* **2019**, *90*, 103030. [CrossRef] [PubMed]
11. Li, X.D.; Li, X.M.; Li, X.; Xu, G.M.; Liu, Y.; Wang, B.G. Aspewentins D–H, 20-nor-isopimarane derivatives from the deep sea sediment-derived fungus *Aspergillus wentii* SD-310. *J. Nat. Prod.* **2016**, *79*, 1347–1353. [CrossRef] [PubMed]
12. Li, X.; Chi, L.P.; Navarro-Vázquez, A.; Hwang, S.; Schmieder, P.; Li, X.M.; Li, X.; Yang, S.Q.; Lei, X.; Wang, B.G.; et al. Stereochemical elucidation of natural products from residual chemical shift anisotropies in a liquid crystalline phase. *J. Am. Chem. Soc.* **2019**. [CrossRef] [PubMed]
13. Kawahara, N.; Nozawa, K.; Nakajima, S.; Kawai, K.I. Emeheterone, a pyrazinone derivative from *Emericella heterothallica*. *Phytochemistry* **1988**, *27*, 3022–3024. [CrossRef]
14. Wang, J.M.; Jiang, N.; Ma, J.; Yu, S.S.; Tan, R.X.; Dai, J.G.; Si, Y.K.; Ding, G.Z.; Ma, S.G.; Qu, L.; et al. Study on absolute configurations of α/α' chiral carbons of thiodiketopiperazines by experimental and calculated circular dichroism spectra. *Tetrahedron* **2013**, *69*, 1195–1201. [CrossRef]
15. Crystallographic data of compounds 1–3 have been deposited in the Cambridge Crystallographic Data Centre as CCDC 1935572, CCDC 1935573 and CCDC 1935571, respectively. Available online: <https://www.ccdc.cam.ac.uk/structures/> (accessed on 13 March 2020).
16. Sheldrick, G.M. *SADABS, Software for empirical absorption correction*; University of Gottingen: Gottingen, Germany, 1996.
17. Sheldrick, G.M. *SHELXTL, Structure determination software programs*; Bruker Analytical X-ray System Inc.: Madison, WI, USA, 1997.
18. Sheldrick, G.M. *SHELXL-97 and SHELXS-97, Program for X-ray Crystal Structure Solution and Refinement*; University of Gottingen: Gottingen, Germany, 1997.
19. Flack, H.D. On enantiomorph-polarity estimation. *Acta Cryst.* **1983**, *39*, 876–881. [CrossRef]
20. Gaussian09, Revision C.01. Available online: <http://gaussian.com/g09citation/> (accessed on 13 March 2020).
21. Liu, G.; Kuang, S.; Cao, R.; Wang, J.; Peng, Q.; Sun, C. Sorafenib kills liver cancer cells by disrupting SCD1-mediated synthesis of monounsaturated fatty acids via the ATP-AMPK-mTOR-SREBP1 signaling pathway. *FASEB J.* **2019**, *33*, 10089–10103. [CrossRef] [PubMed]

